

Quantum resonances of kicked rotor in the position representation

Kush Mohan Mittal* and M. S. Santhanam†

Indian Institute of Science Education and Research, Dr. Homi Bhabha Road, Pune 411 008, India

(Dated: March 13, 2024)

The study of quantum resonances in the chaotic atom-optics kicked rotor system is of interest from two different perspectives. In quantum chaos, it marks out the regime of resonant quantum dynamics in which the atomic cloud displays ballistic mean energy growth due to coherent momentum transfer. Secondly, the sharp quantum resonance peaks are useful in the context of measurement of Talbot time, one of the parameter that helps in precise measurement of fine structure constant. Most of the earlier works rely on fidelity based approach and have proposed Talbot time measurement through experimental determination of the momentum space probability density of the periodically kicked atomic cloud. Fidelity approach has the disadvantage that phase reversed kicks need to be imparted as well which potentially leads to dephasing. In contrast to this, in this work, it is theoretically shown that, without manipulating the kick sequences, the quantum resonances through position space density can be measured more accurately and is experimentally feasible as well.

I. INTRODUCTION

Kicked rotor system, a particle that is periodically kicked by an external sinusoidal field, is a fundamental model of chaotic dynamics in a Hamiltonian system [1, 2]. Atom-optics kicked rotor is an experimentally accessible version of the quantum kicked rotor model implemented by subjecting cold atomic gases to flashing optical lattices [3]. For large kick strengths, classical kicked rotor displays diffusive mean energy growth while in the corresponding quantum regime it is suppressed by quantum interference effects leading to dynamical localization [1, 2, 4]. Such distinct dynamical behaviour in the classical and quantum regime is what makes this system useful to study the quantum to classical transition and decoherence effects. Recently, atom-optics kicked rotor has been employed to demonstrate non-exponential coherence decays and optimal diffusion rates [5]. In general, it has been used widely to study unusual quantum transport scenarios [6], quantum entanglement [7–9] and in quantum metrology for acceleration measurements [10].

From the point of view of atomic interferometry [11] and metrology applications, the quantum resonances in the atom-optics kicked rotor [12, 13] are of special interest. Such resonances are purely quantum effects without any classical analogue. In the kicked rotor system, quantum resonances occur if the scaled Planck's constant is of the form $\hbar = 4\pi\frac{l}{s}$, where l and s are integers. For $s = 1$, time interval between successive kicks is called the Talbot time and the energy of the kicked rotor system grows quadratically due to coherent momentum transfer to the atomic cloud. However, if $s \neq 1$, then an initial state recurs after s kicks, in which the phase added by successive kicks tends to cancel each other. This is called the anti-resonances [14]. Measurement of Talbot time through resonance effects is important for determining

precise values of fine structure constant and hence a crucial ingredient for quantum metrology [15]. The quantum resonances are at the heart of atom interferometers and were experimentally realised using atom-optics kicked rotors [16–18]. One proposal for atom-optics kicked rotor based interferometry relies on manipulating kick sequences in such a way that the N pulses imparted to the atomic cloud are followed by N pulses whose phases differ by π with respect to the former sequence [22]. This is shown to be capable of measuring Talbot time and the local gravitational field [22]. It is also known that quantum resonances are reasonably robust to small amounts of phase noise [23] and amplitude noise [24, 25] in the kick sequences, thus making these systems attractive for interferometric studies and measurement of Talbot time.

Atom optics kicked rotor system can be used to measure Talbot time and it mainly relies on momentum space measurements. The first order effects of perturbation about the Talbot time shows up as a change in the phase of the coefficients in momentum basis. Hence, this effect cannot be detected directly by measuring the momentum distribution of atoms [19, 22]. To measure these effects, a fidelity measurement has been proposed involving the application of phase reversed kicks [19]. In this scheme, N periodic kicked rotor pulse sequences of strength k are followed by the last pulse which will have opposite phase and strength Nk . This is shown to display a sharp resonance peak whose width is proportional to N^{-3} [19] in contrast to mean energy resonant profiles which scales as N^{-2} . This scenario was experimentally observed in a fidelity measurement performed on Bose-Einstein condensate in pulsed external field [20]. Although this was able to capture the first order changes in the phase, experimentally the kick reversal process led to pronounced dephasing. Hence this scheme was not feasible for large kick numbers. Thus, dephasing became an impediment to achieving even sharper resonance peaks.

In order to overcome this deficiency, in this paper, we propose position space measurement and this does not require manipulating the standard pulse sequence imparted to the kicked rotor system. This is motivated by the fact

* E-mail: kush.mohan@students.iiserpune.ac.in

† E-mail: santh@iiserpune.ac.in

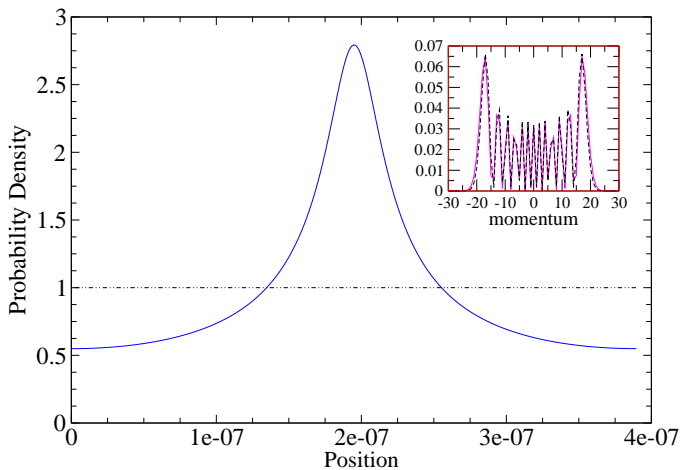


FIG. 1. Position space density after $N = 40$ kicks have been imparted to the initial state evolving under the effect of kicked rotor Hamiltonian. The dotted line corresponds to $\varepsilon = 0$ and solid line to $\varepsilon = 10^{-8}$. The inset shows the momentum space density for the same values of ε as the main figure. Note the pronounced difference between the cases of these two values of ε observed in the position representation, but not in the case of momentum representation.

that if the kick period differs from the Talbot time by $\varepsilon \ll 1$, then to first order, the resulting effect shows up directly in the spatial distribution of atoms as a narrower initial peak about the Talbot time without the requirement of the kick reversal process. On the other hand, in the momentum space, the effect is not distinct from the case with $\varepsilon = 0$. Hence, quantum resonance is better analysed in the position representation. This is illustrated in Fig. 1. In this, the position space density is displayed for fixed values of $\varepsilon = 0$ and 10^{-8} after $N = 40$ kicks are imparted. Clearly, in comparison with the case of $\varepsilon = 0$, for small deviation from Talbot time, position density shows pronounced difference. In the momentum representation (shown in the inset of Fig. 1), the probability densities for $\varepsilon = 0$ and 10^{-8} after $N = 40$ kicks do not show any perceptible difference. The analysis presented in this paper is motivated by this observable effect in position space as well as the fact that the experiments using optical mask techniques can directly probe position space density of cold atomic cloud [21]. Further, we also extend the results in Ref. [26] to derive analytical result for change in position density around the Talbot time. We compare the analytical results with the simulations.

II. QUANTUM RESONANCES IN THE δ -KICKED ROTOR

Kicked rotor system is experimentally realized using ultra-cold atoms in optical lattices. In this, the periodic kicks are imparted using two far-detuned counter propagating laser beams. The pulse is considered to be in the short pulse or Raman-Nath limit, *i.e.*, the evolution of

the atomic cloud during the pulse duration is negligible. In the ideal limit of delta kicks the system is described by the dimensionless Hamiltonian [4] given by

$$\hat{H} = \frac{\hat{P}^2}{2M} + K \cos \hat{X} \sum_{n=0}^{N-1} \delta(t - n). \quad (1)$$

where we have assumed that a total of N kicks are imparted to the atomic cloud. In this, K is the kicking strength, k_L is the wave number of the standing wave, T is periodicity of the kicks. Both \hat{X} and \hat{P} are the scaled canonical variables. The corresponding evolution operator is

$$\hat{U} = \exp\left(-i\frac{K}{\hbar_s} \cos X\right) \exp\left(-i\frac{P^2}{2\hbar_s}\right), \quad (2)$$

in which $\hbar_s = 4\hbar k_L^2 T/M$ represents the scaled Planck's constant. The evolution operator splits into the kick and the free evolution part due to the δ -kicks. As the kicking potential is spatially periodic, the eigenstates have a Bloch wave structure. Hence, an initial state $|P_o\rangle$ corresponding to definite momentum, under the action of the evolution operator, gets mapped to states of the form $|P_o + m\hbar_s\rangle$, with m being an integer. In the analysis presented below, we shall be considering the case where the particles are initially in the zero momentum state, *i.e.*, $|P_o = 0\rangle$. It must be noted that if the profile of the initial state has a width due to finite temperature effects, then the temporal evolution of the initial state strongly deviates from that corresponding to $|P_o = 0\rangle$ for longer times. This time-scale is inversely proportional to the width of the initial momentum distribution [27]. In experiments, at longer times (more kicks) the dephasing effects become significant as well. Hence, the analysis presented here is valid until dephasing becomes pronounced even if initial states are not ideal. Further, the results of numerical simulations shown in this were performed for an effective kick strength of $K/\hbar_s = 0.485$ and λ_L corresponding to a wavelength of 780 nm.

Considering this, we can write the state of the particle at any arbitrary time in the form,

$$\Psi(X) = \frac{1}{\sqrt{2\pi}} \sum_{m=-\infty}^{\infty} \psi(m) e^{imX}. \quad (3)$$

Quantum resonance is characterized by the value of $\hbar_s = 4\pi l$, $l > 0$ is an integer. Then, the free evolution part of \hat{U} given in Eq.(2) becomes $\exp(-i2\pi m^2 l)$, effectively an identity operator. For this choice of \hbar_s , the kick period T is referred to as the Talbot time T_b corresponding to the physical picture that the kicks accumulate phases in a coherent manner [26]. In the analysis that follows, we compute the change in $\Psi(X)$ due to small perturbation in the Talbot time T_B . Unlike the earlier studies in momentum representation, we study the resonances in position representation.

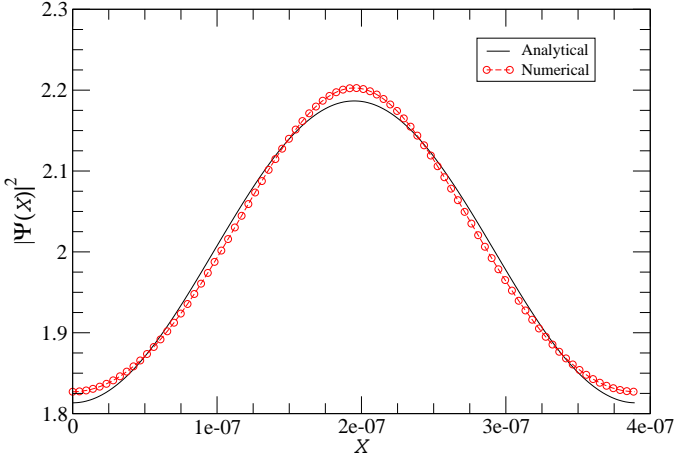


FIG. 2. Position space density after $N = 5$ kicks have been imparted to the initial state evolving under the effect of kicked rotor Hamiltonian. The deviation from Talbot time is $\varepsilon = 10^{-7}$. The solid curve is the analytical result in Eq. 12 and symbols are the numerically computed result.

III. PERTURBATION ABOUT THE TALBOT TIME

As pointed out earlier, we assume that only N kicks are to be imparted. In the experimental context, depending on the parameters of the set-up, typically the number of kicks do not exceed a few hundred in units of kick period. Let $\Psi(X, t-1)$ represent the state at time $t-1$ and corresponds to the time when the $(N-1)^{th}$ kick is just applied. Following this, the free evolution operator is applied to it for time $t = T_B + \varepsilon$ where $\varepsilon \ll 1$ is a small perturbation about the Talbot time. This leads to

$$\Psi(X, t^-) = \exp\left(-i\frac{P^2}{2\kappa}\right)\Psi(X, t-1), \quad (4)$$

in which t^- denotes the state just before the N^{th} kick is applied. Now, as discussed earlier, $P = m\hbar_s$ and it is evident that for small perturbations about the Talbot time the scaled Planck's constant becomes $\hbar_s = 4\pi l(1 + \frac{\varepsilon}{T_B})$. Substituting these values for P and \hbar_s in Eq.(4), we get

$$\Psi(X, t^-) = \exp\left(-i\frac{m^2}{2}4\pi l\left(1 + \frac{\varepsilon}{T_B}\right)\right)\Psi(X, t-1). \quad (5)$$

The exponential term can be split into two parts; one corresponding to the ideal Talbot time condition and other corresponding to the perturbation. For $\varepsilon \ll 1$, the exponential is expanded as a Taylor series and terms of order ε^2 and higher are discarded. We consider the primary resonance by taking $l = 1$, and this leads to

$$\begin{aligned} \Psi(X, t^-) &= e^{-i2\pi m^2} \Psi(X, t-1) \exp\left(-i2m^2\pi\frac{\varepsilon}{T_B}\right) \\ &= \Psi(X, t-1) - i2m^2\pi\frac{\varepsilon}{T_B}\Psi(X, t-1) \end{aligned} \quad (6)$$

Using Eq.(3), $\Psi(X, t^-)$ can be rewritten as

$$\begin{aligned} \Psi(X, t^-) &= \Psi(X, t-1) - \\ &\frac{1}{\sqrt{2\pi}} \sum_{m=-\infty}^{\infty} \psi(m, t-1) e^{imX} \left(i2m^2\pi\frac{\varepsilon}{T_B}\right) \end{aligned} \quad (7)$$

To analyze the first order effect of the perturbation, the position space density is obtained as

$$\begin{aligned} |\Psi(X, t^-)|^2 &= |\Psi(X, t-1)|^2 - \frac{2\pi i\varepsilon}{\sqrt{2\pi}T_B} \\ &\sum_{m=-\infty}^{\infty} m^2 [\Psi^*(X, t-1)\psi(m, t-1)e^{imX} + \\ &\Psi(X, t-1)\psi^*(m, t-1)e^{-imX}], \end{aligned} \quad (8)$$

in which only the terms first order in ε are retained. The first term on the right hand side corresponds to the probability density at time $t-1$ which already includes the effect of small perturbation about Talbot time. The rest of the terms are first order corrections at N -th kick. Using Eq.(3) again, the correction terms appearing in Eq.(8) can be written as

$$\begin{aligned} &\sum_{n=-\infty}^{\infty} \sum_{m=-\infty}^{\infty} \frac{im^2\varepsilon}{T_B} \left(\psi^*(n, t-1)\psi(m, t-1)e^{i(m-n)X} + \right. \\ &\left. \psi(n, t-1)\psi^*(m, t-1)e^{i(n-m)X} \right). \end{aligned} \quad (9)$$

It is evident that the terms for which $n = m$ cancel each other and the summation is left with terms with $n \neq m$. Thus, the corrections can equivalently be written as,

$$\begin{aligned} &\sum_{m=-\infty}^{\infty} \sum_{n>m} 2 \operatorname{Re} \left[\frac{1}{2\pi} \psi^*(n, t-1)\psi(m, t-1)e^{i(m-n)X} \right. \\ &\left. \left(i(n^2 - m^2) \frac{2\pi\varepsilon}{T_B} \right) \right] \end{aligned} \quad (10)$$

where $\operatorname{Re}(\cdot)$ represents the real part. Since we are working upto first order in ε , the amplitude ψ in Eq.(10) corresponds to that when the Talbot condition is met. Hence they can be written in terms of n -th order Bessel function $J_n(\cdot)$ as $\psi(n, t-1) = (-i)^n J_n((N-1)\phi_d)$ [28] where $\phi_d = K/\hbar_s$ at time $t-1$ when the $(N-1)^{th}$ kick has been applied. This leads to the expression for the correction term $C_N(\varepsilon)$:

$$\begin{aligned} C_N(\varepsilon) &= \frac{1}{\pi} \sum_{m=-\infty}^{\infty} \sum_{n>m} \operatorname{Re} \left[e^{i(m-n)X} (n^2 - m^2) \frac{2\pi i\varepsilon}{T_B} \right. \\ &\left. i^n J_n((N-1)\phi_d) (-i)^m J_m((N-1)\phi_d) \right] \end{aligned} \quad (11)$$

In this, $J_m(\cdot)$ is the Bessel function of order m with real argument. Thus, the probability density under the first order approximation can be finally written as,

$$|\Psi(X, t^-)|^2 = |\Psi(X, t-1)|^2 + C_N(\varepsilon). \quad (12)$$

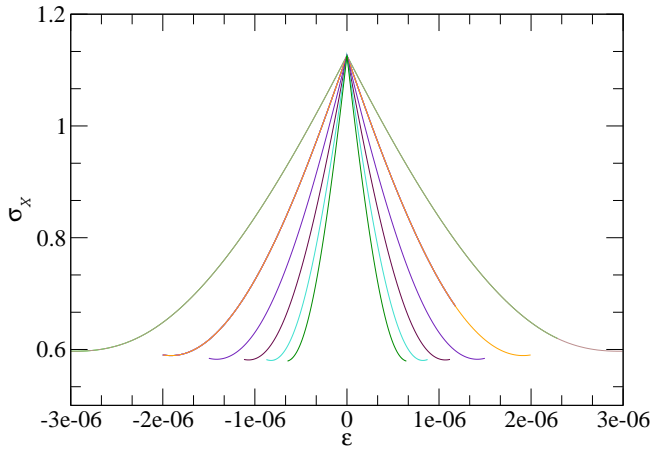


FIG. 3. The numerically computed standard deviation σ_X of the probability density function as a function of perturbation about Talbot time ε for a fixed kick number. It is displayed for the kick numbers $N = 5$ (outer most curve) to $N = 10$ (inner most curve). The value of σ_X decreases with increase in the kick number.

Physically, the effect of kick is to give a phase factor of $\exp(-i\frac{K}{\hbar_s} \cos X)$. This does not affect the probability density in position basis, but leads to occupancy of higher momenta states which in turn affects the perturbation term. It is clear that Eq.(12) forms a recursive equation connecting Ψ at successive kicks and complete analytical though cumbersome approximation can be found recursively.

IV. POSITION SPACE ANALYSIS

In Fig. 2, perturbation based analytical result obtained in Eq.(12) is compared with the numerical simulations for $\varepsilon = 10^{-7}$ and $N = 5$ kicks. The analytical result is calculated recursively starting from momentum eigenstate $p_0 = 0$ at $t = 0$. The kicked rotor Hamiltonian is evolved with kick strength $\phi_d = K/\hbar_s = 0.485$. There is a reasonably good agreement between the analytical and the numerical position space distribution. In particular, the quantity of interest, the standard deviation of the distribution, is well captured by the analytical result.

For the present purposes, the quantity of interest would be the sharpness of the resonance in position space density $|\Psi(X)|^2$. This is conveniently measured using the standard deviation denoted by σ_X . It is anticipated that as the kick period deviates from Talbot time, as quantified by ε , the position space density will evolve from a uniform profile at $N = 0$ (shown in Fig. 1) to a narrow profile as $N \gg 1$. The width σ_X of this profile will decay with increasing kick number. As is evident from the numerical results in Fig. 3, as the number of kicks increase, the width does indeed decrease. It takes a power-law form $\sigma_X \propto N^{-\gamma}$, and the exponent γ is estimated by regression to be 2.10.

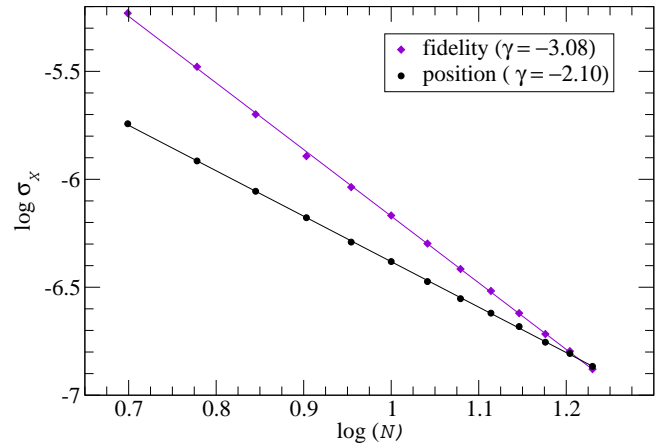


FIG. 4. The width σ of distribution about the Talbot time as a function of kick number for fidelity analysis (reported in [19]) and the position space analysis studied in this paper. The symbols are the simulation results and the solid lines represent best-fit lines. The slope for fidelity analysis is estimated to be $\gamma = -3.08$ while for the position space analysis it is $\gamma = 2.10$.

It must be noted that the width in the case of fidelity based analysis scales with N whose exponent is $\gamma \approx -3.0$ [19]. Thus, approximately, the width of the distribution for position space analysis scales as $1/N^2$ whereas for fidelity analysis it scales as $1/N^3$. Notice also that in general the width of position space based method starts from far lower width in comparison to the fidelity method. It turns out that till $N = 16$ kicks, the position space distribution has lesser σ than that of fidelity approach and hence can potentially lead to better Talbot time measurement.

However, one significant problem with the fidelity technique is the requirement of kick reversal process, which can potentially lead to dephasing. This implies that, for a fair comparison of both these approaches, if position space analysis presented here applied M kicks, then fidelity technique will require $2M$ kicks, *i.e.*, M normal kicks plus M phase reversed kicks, to be applied. If this is taken into account, then for identical *total* number of kicks applied, it is clearly seen that position space density based analysis of quantum resonance far outperforms the fidelity based approach.

V. CONCLUSIONS

The quantum resonances in the position space representation of the atom optics kicked rotor system is analysed in this paper. In the kicked rotor system, quantum resonances can be observed when the scaled Planck's constant is given by, $\hbar = 4\pi l$, where l is an integer. Thus, this analysis provides theoretical results for the measurement of Talbot time in position space representation. Generally, the atom-optics based kicked rotor

experiments perform measurements in momentum space. However, the central result of this paper is that the quantitative signatures of quantum resonances, and hence the Talbot time, are better inferred from position space, rather than in momentum space, representation.

For this purpose, we have analytically obtained the first order changes in the position space density of the evolving atomic cloud about Talbot time. The basic idea in this work is to capture the changes which occur in the phase in momentum space directly by measuring the probability distribution in position space. This can be further extended to various other setup and problems as an efficient alternative to fidelity based treatment in order to capture the phase information. The latter requires

kick sequence manipulation which often lead to dephasing effects of the atomic cloud within a few kicks. It is shown that the position space analysis can be more accurate in measuring the Talbot time. Further, it is much more experimentally feasible than the fidelity treatment quantum resonances based on momentum space analysis. In this position representation approach, the width of the quantum resonances scale approximately as N^{-2} , where N is the number of kicks. Significantly, this does not require manipulating the kick sequence (as is normally done for fidelity based approaches). As experimental techniques for directly probing position space density through optical mask techniques are available [21], this work might lead to direct Talbot time measurements.

-
- [1] F. Haake, *Quantum signatures of chaos* (Springer Science & Business Media, Berlin Heidelberg 2013).
 - [2] F. M. Izrailev, Phys. Rep. **196**, 299 (1990).
 - [3] F. L. Moore, J. C. Robinson, C. Bharucha, P. E. Williams, and M. G. Raizen, Phys. Rev. Lett. **73**, 2974 (1994).
 - [4] L. Reichl, *The Transition to chaos : Conservative classical systems and quantum manifestations*, (Springer, 2004).
 - [5] S. Sarkar, S. Paul, C. Vishwakarma, S. Kumar, G. Verma, M. Sainath, Umakant D. Rapol, and M.S. Santhanam, Phys. Rev. Lett. **118**, 174101 (2017).
 - [6] I. Manai, J. F. Clement, R. Chicireanu, C. Hainaut, J. C. Garreau, P. Szriftgiser, and D. Delande, Phys. Rev. Lett. **115**, 240603 (2015); F. Revuelta, R. Chacón, and F. Borondo, Phys. Rev. E **98**, 062202 (2018); S. Longhi, Phys. Rev. A **95**, 012125 (2017).
 - [7] K. Furuya, M. C. Nemes, and G. Q. Pellegrino, Phys. Rev. Lett. **80**, 5524 (1998).
 - [8] J. N. Bandyopadhyay and A. Lakshminarayan, Phys. Rev. Lett. **89**, 060402 (2002).
 - [9] F. Matsui, H. S. Yamada, and K. S. Ikeda, EPL **114**, 60010 (2016).
 - [10] R. A. Horne, R. H. Leonard, and C. A. Sackett, Phys. Rev. A **83**, 063613 (2011); S. Chai, J. Fekete, and M. F. Andersen, Phys. Rev. A **98**, 063614 (2018).
 - [11] K. Hornberger, S. Gerlich, P. Haslinger, S. Nimmrichter, and M. Arndt, Rev. Mod. Phys. **84**, 157 (2012).
 - [12] F. M. Izrailev and D. L. Shepelyanskii, Theor. Math. Phys. **43**, 553 (1980).
 - [13] S. Wimberger, I. Guarneri and S. Fishman, Nonlinearity **16**, 1381 (2003).
 - [14] I. Dana, E. Eisenberg and N. Shnerb, Phys. Rev. E **54**, 5948 (1996).
 - [15] L. Pezzé, A. Smerzi, M. K. Oberthaler, R. Schmied, and P. Treutlein, Rev. Mod. Phys. **90**, 035005 (2018).
 - [16] A. Tonyushkin and M. Prentiss, Phys. Rev. A **78**, 053625 (2008).
 - [17] C. Ryu et. al., Phys. Rev. Lett. **96**, 160403 (2006).
 - [18] M. Lepers, V. Zehnlé, and J. C. Garreau, Eur. Phys. J. D **63**, 449 (2011).
 - [19] P. McDowall, A. Hilliard, M. McGovern, T. Grúnzweig, M. F. Andersen, New J. Phys. **11**, 123021 (2009).
 - [20] I. Talukdar, R. Shrestha, and G. S. Summy, Phys. Rev. Lett. **105**, 054103 (2010).
 - [21] A. Turlapov, A. Tonyushkin, and T. Sleator, Phys. Rev. A **71**, 043612 (2005).
 - [22] B. Daszuta and M. F. Andersen, Phys. Rev. A **86**, 043604 (2012).
 - [23] D H White, S K Ruddell and M D Hoogerland , New J. Phys. **16**, 113039 (2014).
 - [24] M. Sadgrove, S. Wimberger, S. Parkins and R. Leonhardt, Phys. Rev. E. **78**, 025206 (2008); M. Sadgrove, T. Mullins, S. Parkins and R. Leonhardt, Physica E **29**, 369 (2005).
 - [25] S. Brouard and J. Plata, J. Phys. A : Math. Gen. **36**, 3745 (2003).
 - [26] M. Lepers, V. Zehnle, and J. C. Garreau, Phys. Rev. A **77**, 043628 (2008).
 - [27] M. Saunders, P. L. Halkyard, K. J. Challis, and S. A. Gardiner, Phys. Rev. A **76**, 043415 (2007).
 - [28] A. Cuyt A, V. Petersen, B. Verdonk, H. Waadeland and W. B. Jones, *Handbook of Continued Fractions for Special Functions* (Springer, Berlin, 2008).